

# Characterization of interfaces: Lessons from the past for the future of perovskite solar cells

Wanlong Wang<sup>1, ‡</sup>, Dongyang Zhang<sup>2, ‡</sup>, Rong Liu<sup>1, †</sup>, Deepak Thrithamarassery Gangadharan<sup>2</sup>, Furui Tan<sup>1, †</sup>, and Maksud I. Saidaminov<sup>2, †</sup>

<sup>1</sup>Key Laboratory of Photovoltaic Materials, Henan University, Kaifeng 475004, China

<sup>2</sup>Department of Chemistry, Department of Electrical & Computer Engineering, and Centre for Advanced Materials and Related Technologies (CAMTEC), University of Victoria, Victoria, British Columbia V8P 5C2, Canada

**Abstract:** A photovoltaic technology historically goes through two major steps to evolve into a mature technology. The first step involves advances in materials and is usually accompanied by the rapid improvement of power conversion efficiency. The second step focuses on interfaces and is usually accompanied by significant stability improvement. As an emerging generation of photovoltaic technology, perovskite solar cells are transitioning to the second step of their development when a significant focus shifts toward interface studies and engineering. While various interface engineering strategies have been developed, interfacial characterization is crucial to show the effectiveness of interfacial modification. Here, we review the characterization techniques that have been utilized in studying interface properties in perovskite solar cells. We first summarize the main roles of interfaces in perovskite solar cells, and then we discuss some typical characterization methodologies for morphological, optical, and electrical studies of interfaces. Successful experiences and existing problems are analyzed when discussing some commonly used methods. We then analyze the challenges and provide an outlook for further development of interfacial characterizations. This review aims to evoke strengthened research devotion on novel and persuasive interfacial engineering.

**Key words:** interface; perovskite solar cells; characterization methods

**Citation:** W L Wang, D Y Zhang, R Liu, D T Gangadharan, F R Tan, and M I Saidaminov, Characterization of interfaces: Lessons from the past for the future of perovskite solar cells[J]. *J. Semicond.*, 2022, 43(5), 051202. <https://doi.org/10.1088/1674-4926/43/5/051202>

## 1. Introduction

The simplest solar cell is a sandwich of at least four materials (front electrode, p- and n-semiconductors, and back electrode) with at least five interfaces (three between materials, and front and back surfaces). As solar cells are developed, they will involve more layers and interfaces: for instance, the best Si solar cell consists of p-n junction layers and passivating interfaces<sup>[1–3]</sup>. Engineering of interfaces should count for electrical, chemical, optical and thermal properties of two adjacent materials, and is important for the overall device performance.

Interface engineering has played a significant role in mature photovoltaic technologies (Fig. 1). For example, the Si solar cell with a record efficiency of 26.7% PCE was achieved by extensive interface passivations: an n-type crystalline Si (c-Si) was passivated by p<sup>+</sup> heterojunction layer stack (i.e., a-Si:H layer deposition followed by p:a-Si:H layer deposition) from one side and n<sup>+</sup> heterojunction layer stack (i.e., a-Si:H layer deposition followed by n-type thin-film Si layer deposition) from the other side<sup>[4]</sup>. The present champion CIGS cell with a PCE of 22.9% was achieved in part due to Cs surface passivation<sup>[5]</sup>. In CdTe cells with a PCE of 20%, Se or S doped

CdTe<sub>1-x</sub>Se<sub>x</sub> or CdTe<sub>1-x</sub>S<sub>x</sub> as the light active layer has neutralized the surface defects of CdTe<sup>[6, 7]</sup>. Similarly, GaAs solar cell with the highest PCE of 29.1% benefited from suppressing nonradiative recombination processes at the two GaAs/buffer interfaces<sup>[8]</sup>. Interfacial engineering greatly contributes to the development of state-of-the-art performance of traditional photovoltaic techniques.

For the emerging perovskite photovoltaics, halide perovskite now undergoes rapid advance to a higher efficiency, and a better stability and scalability<sup>[10–14]</sup>, during which interface modulation also played a crucial role in improving the efficiency that has reached state-of-the-art value of 25.5%<sup>[9]</sup>. Looking back at the development of perovskite solar cells, one could note that the major work in early stage of perovskite photovoltaics mainly focused on optimization in perovskite composition and film formation (Fig. 1 black dots). In the last few years, the efficiency record was frequently obtained through various interface engineering, such as fluorine terminated hole-transport layer (HTL) to tune the interfacial energy-level alignment<sup>[15]</sup>, PEAI passivated interface between perovskite and HTL<sup>[16]</sup>, and multifunctional passivation of interface with graded dimensional perovskite<sup>[17]</sup>, and so on. It is reasonable to speculate that, based on sufficient optimization on perovskite component, a major focus will shift toward interface engineering to maximize the efficiency further and stabilize devices. Therefore, it will be of profound importance to fully understanding how the interfaces will influence the fundamental mechanism of perovskite devices,

Wanlong Wang and Dongyang Zhang contributed equally to this work.

Correspondence to: R Liu, [liurong@pkusz.edu.cn](mailto:liurong@pkusz.edu.cn); F R Tan,

[ftan@henu.edu.cn](mailto:ftan@henu.edu.cn); M I Saidaminov, [msaidaminov@uvic.ca](mailto:msaidaminov@uvic.ca)

Received 12 OCTOBER 2021; Revised 24 NOVEMBER 2021.

©2022 Chinese Institute of Electronics

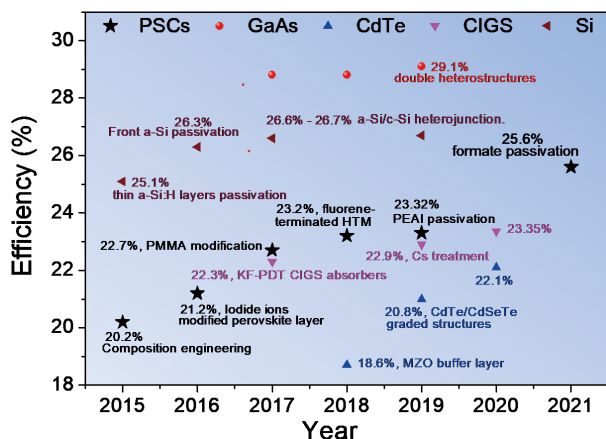


Fig. 1. (Color online) Efficiency evolution of different solar cells. Interface engineering has recently played an increasingly important role in obtaining a higher efficiency for each cell.

which greatly depends on a deep and full characterization on interfaces in perovskite devices.

However, it is known that the interface is formed between two heteromaterials and usually spans over only several atomic layers<sup>[18, 19]</sup>. This makes direct and reliable measurements on this precise location to some extent difficult. To get persuasive and reliable information on future interface modification, it is necessary to take look back at the correlated interface-characterization process with various characterization tools. In this review, we summarize the past interface-related characterizations on perovskite solar cells. We first summarize the main roles of interfaces that should be considered before a suitable interface-characterization method is chosen. We then discuss interface analysis methods those were used during interface modification on the morphological, optical, and electrical improvements of photovoltaic films. Prospects and suggestions are given based on detailed analysis and comparison on the existed characterization methods. We expect that this review will stimulate new strategies for interface engineering of perovskite solar cells, leading to the improvement of efficiency and stability beyond the state-of-the-art.

## 2. The role of interfaces for perovskite solar cells

It is known that interface of a perovskite solar cell impacts the performance of the device (e.g., the excitation information, separation, and recombination). Furthermore, the degradation of a device is also highly sensitive to the interface. An experimental point of view showed that interfacial defects in PSCs were relevant with such these key issues, such as instability<sup>[20, 21]</sup>, ion migration<sup>[22, 23]</sup>, current-voltage hysteresis<sup>[24–26]</sup>, giant photovoltaic effect switchable by electric field<sup>[27, 28]</sup>, and formation of n–i–p structures<sup>[29, 30]</sup>.

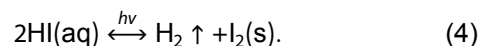
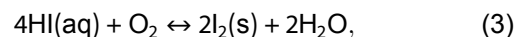
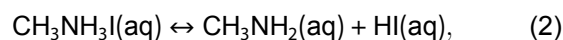
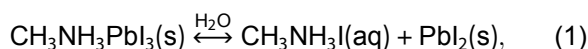
### 2.1. Oxygen infiltration

Interfaces in PSCs affect their chemical stability<sup>[13, 31–38]</sup>. Air-induced material stability issues are common because oxygen and moisture prefer to infiltrate into perovskite devices through these planar interfaces. Oxygen infiltration mainly has two impacts. The first impact is to cause oxidation of subvalence metal ions, such as Sn<sup>2+</sup> and Ge<sup>2+</sup> to their stable states, which usually deteriorates the performance of photovoltaic devices<sup>[39–41]</sup>. The second impact is to partially oxidize the traditionally adopted organic HTLs with dopants to in-

crease their conductivity<sup>[42, 43]</sup>, benefitting the photovoltaic performance of perovskite solar cells that are based on Pb (but not Sn or Ge).

### 2.2. Humidity corrosion

Compared to the oxygen penetration at the interface, moisture diffusion along the interface seems to be more detrimental. A great deal of research has reported performance degradation due to interface-related moisture corrosion<sup>[44, 45]</sup>. For polycrystalline organic-inorganic hybrid perovskite films, moisture induced component decomposition usually starts at interfaces and grain boundaries<sup>[46, 47]</sup>. Even for air stable inorganic perovskite, high humidity will also cause a phase transition that degrades the optoelectronic properties of perovskite films<sup>[48, 49]</sup>. Because H<sub>2</sub>O and O<sub>2</sub> coexist in air, perovskite film or devices working in this atmosphere would undergo accelerated degradation caused by both of these species. H<sub>2</sub>O would first decompose perovskite to produce organohalide, after which O<sub>2</sub> will further react with hydrohalic acid to generate halogen (reactions (1) to (4)), which can be observed in absorption spectrum<sup>[45, 50, 51]</sup>. Therefore, interface engineering by incorporating hydrophobic groups or materials at interfaces has become a common strategy<sup>[52–56]</sup>.



### 2.3. Electronic behavior

As a key part of multilayer optoelectronic devices, the interfaces in perovskite solar cells mainly play a role in charge transfer extraction. An efficiency gap may result from nonradiative recombination (Fig. 2), energy mismatch and optical losses at the interface. During the transfer of charge between perovskite and CTL, a recombination of the carrier would occur. Interface engineering is required to reduce interfacial recombination losses<sup>[57–59]</sup>. For example, Tan *et al.* developed contact passivation strategy at ETL/perovskite planar interface by introducing a Cl coordinator to modulate the charge dynamics for improved solar cells<sup>[60]</sup>. Many other interfacial modifiers (e.g., bifunctional molecules and intrinsic ultrathin layers, etc.) have also been reported for interfacial passivation<sup>[61–64]</sup>.

For charge transfer extraction, it is necessary to have a suitable energy-level alignment between transport layers and perovskite. This is vital to solar cell parameters, such as photovoltage and fill factor (FF)<sup>[65, 66]</sup>. Type-II band alignment is needed for contact at the ETL/perovskite or HTL/perovskite interface. In particular, the conduction band minimum (CBM) of perovskite should be higher than that of ETL, while the valence band maximum (VBM) should be lower than that of HTL. Experimental results show the differences in CBM between perovskite and ETL or VBM between perovskite and HTL should be around 0.2 eV for efficient charge extraction<sup>[67, 68]</sup>. A small offset leads to low driven built-in potential, causing

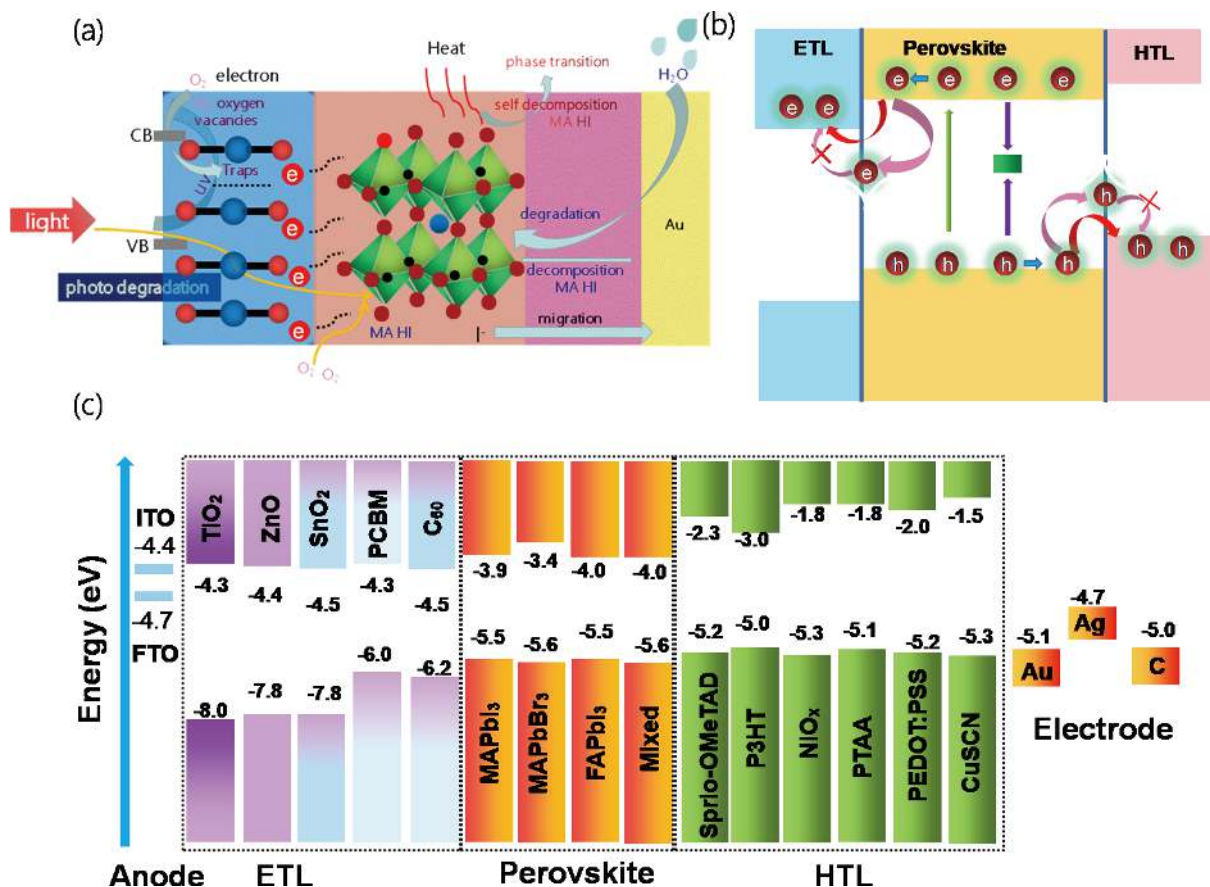


Fig. 2. (Color online) (a) Perovskite crystal structure, Schottky defect, Frenkel defect and ion migration through interfaces. (b) Schematic illustration of photo-generation and, diffusion and transfer of charges at interfaces, trap-assisted nonradiative recombination (due to intrinsic defects and impurities at interfaces) and back transfer and interface recombination. (c) Energy band alignment of some typical materials used in perovskite solar cells.

an accumulation of carriers at interfaces accompanied by severe recombination at interfaces. Meanwhile, a band offset that is too large would cause excess energy loss, which would decrease the  $V_{oc}$  and FF<sup>[69, 70]</sup>. Energy levels can be controlled through chemical doping or compositional alloying<sup>[71–78]</sup>. For example, Sb-doped SnO<sub>2</sub> forms a bilayer ETL of Sb-SnO<sub>2</sub>/SnO<sub>2</sub> with cascade energy alignment promoting high power conversion efficiency<sup>[79]</sup>. Schulz *et al.* measured band bending at the interface between MAPbX<sub>3</sub> and Spiro-OMeTAD<sup>[80]</sup>. The VBM differences of perovskite and Spiro-OMeTAD is 0.4 eV for MAPbI<sub>3</sub>, 0.3 eV for MAPbI<sub>3-x</sub>Cl<sub>x</sub>, and 0.8 eV for MAPbBr<sub>3</sub>, resulting in different  $V_{oc}$  of 1.0, 1.1, and 0.9 V, respectively. Although a slight difference was found between the theoretical and experimental results, appropriate energy-level alignment is pivotal to minimizing  $V_{oc}$  losses at the junction.

### 3. Interface characterization

Because the interfaces are ultrathin—probably within several atoms—and are deeply buried inside the device, it is difficult to carry out direct measurements on these parts. However, because of its importance, some characterization methods have been developed. In this part, we focus on some important characterization process that can reflect the morphological, optical, and electrical information of interfaces. We note that this is not an exhaustive list of characterization tools, but purposely covers the most relevant ones that

might be useful for direct or indirect investigation of interfaces.

#### 3.1. Morphology and composition characterization

Modern scanning electron microscopes (SEMs) have resolutions down to 1 nm. In SEMs, the fast incoming electrons supply energy to the atomic outer-shell electrons in the specimen, which is sufficient for the atomic electron to be released as a “secondary electron” (SE) whose images mainly show the surface structure (topography) of the specimen<sup>[81–83]</sup>. However, by measuring the cross-section of a layered sample that contains some buried interfaces, we can directly obtain some morphological information about part of interfaces. For example, when investigating the effect of appropriate amount of PbI<sub>2</sub> on PSCs performance, the PbI<sub>2</sub> phase can be tracked at perovskite GBs and interfaces (Fig. 3(a))<sup>[84]</sup>. It can be seen that PbI<sub>2</sub> is squeezed into GBs by the perovskite grain growth during the perovskite annealing process. In addition, cross-sectional SEM is especially useful when studying nanostructured interfaces between perovskite and heteromaterials. Take nanorod arrays ETL as an example, SEM images can clearly show the infiltration of perovskite into this nanostructure to evaluate the physical contact quality of heterointerfaces<sup>[85–88]</sup>. Therefore, SEM characterization has become a common and important method to directly “see” interfaces.

Although obtained by optical measurements, photoluminescence (PL) mapping of a perovskite film can reflect the mor-



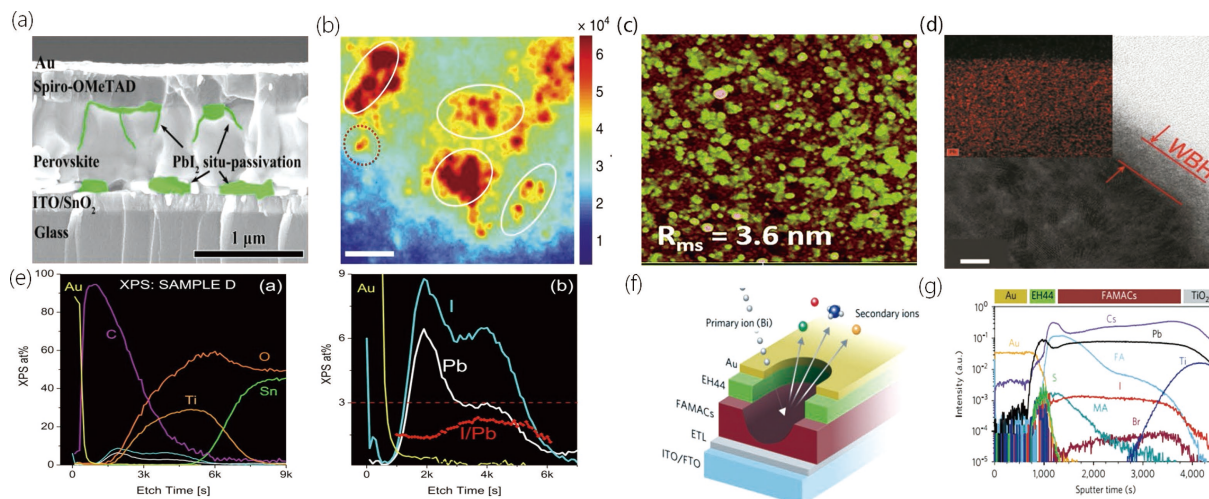


Fig. 3. (Color online) Interface material characterization methods. (a) Cross-section SEM image of PSCs showing excess of  $\text{PbI}_2$  at interfaces. Reproduced with permission from Ref. [84]. Copyright 2019, ACS. (b) Photoluminescence mapping image showing the crystallization of perovskite from the pre-embedded perovskite seeds. Reproduced with permission from Ref. [89]. Copyright 2018, Nature. (c) AFM image of  $\text{TiO}_2$ . Reproduced with permission from Ref. [90]. Copyright 2020, RSC. (d) Cross-sectional HRTEM imaged wide band gap perovskite near the surface. Scale bars:  $1 \mu\text{m}$ . Reproduced with permission from Ref. [91]. Copyright 2019, Nature. (e) XPS depth profiles for cross-sectional characterization. Reproduced with permission from Ref. [95]. Copyright 2015, ACS. (f) and (g) Schematic illustration and measurement results from TOF-SIMS characterization. Reproduced with permission from Ref. [103]. Copyright 2018, Nature.

phological and compositional information of the film, especially when the perovskite films contain multi-phases that show different in-situ PL properties. Different PL intensity and PL wavelengths usually indicate different phase distributions. Therefore, this characterization could be used to study the phase and crystallization properties in the hybrid. Zhao *et al.* studied the mixture of a perovskite solution and  $\text{PbI}_2$ , and proved that the perovskite solution behaved as dispersed seed that showed distinct PL phenomenon in the  $\text{PbI}_2$  matrix. When fabricating the perovskite film by a typical two-step method, the as-existed perovskite seed benefited the crystallization of perovskite with large size. The entire process can be clearly demonstrated by in-situ PL mapping properties of the films (Fig. 3(b))<sup>[89]</sup>.

An atomic force microscope (AFM) is a useful instrument with high atomic resolution that can detect the morphological properties of various materials and samples in the nanometer scale. Compared with a conventional microscope, AFM has the advantage of observing the sample surface with high magnification under atmospheric conditions. It can be used to detect the three-dimensional image of a sample's surface. The roughness calculation, thickness, step width, block diagram and granularity analysis can also be obtained for the 3D morphology image. For example, Methawee Nukunudompanich *et al.* used different methods to prepare  $\text{TiO}_2$  electron transport layers and used AFM to characterize the surface roughness. The growth mechanism of perovskite grain on ETLs with different roughness was thus obtained based on the preliminary AFM characterization results at the interfaces (Fig. 3(c))<sup>[90]</sup>.

A transmission electron microscope (TEM) can be used to observe fine structures smaller than  $0.2 \mu\text{m}$  that cannot be seen under an optical microscope. These structures are called submicroscopic structures or ultrastructures. Because electrons are easily scattered or absorbed by objects, the penetration is low, and the density and thickness of samples will af-

fect the final imaging quality. Therefore, ultrathin perovskite sections with a thickness within several tens of nanometers should be prepared. For interface characterization by TEM, usually cross-sectional sample containing interface part should be prepared and precisely targeted during TEM measurements. Like SEM, TEM is also a direct way to "see" the interface. For example, by high resolution TEM (HRTEM), the interfacial region could be tested to get useful information, such as thickness, location and, if aided by high-angle annular dark-field (HAADF) scanning TEM, the content of a certain atom (Fig. 3(d))<sup>[91]</sup>.

X-ray photoelectron spectroscopy (XPS) is a very sensitive tool to characterize the composition of a film<sup>[92–94]</sup>. Through X ray irradiation, the excited electrons from inner orbital of an atom can be collected and analyzed to get information about different atoms. Because the effective depth from XPS measurement is as small as ten nanometers, direct research on buried interfaces is impossible just from one-time XPS measurement. Luckily, this sensitive method can be combined with physical etching of the sample to measure it on different depths. To obtain more quantitative information of elements, XPS depth was used to analyze the sample. Usually, the in-depth distribution of the atomic species percentages is shown as a function of the sputtering time (Fig. 3(e)), providing the content variation of targeted elements (such as I/Pb) at different depths<sup>[95, 96]</sup>.

Time-of-flight secondary ion mass spectrometry (TOF-SIMS) is another useful method to measure the chemical distribution of the nanocomposite, the interface degradation and ion migration in the device<sup>[97–99]</sup>. Unlike XPS depth measurement where SEs are excited and detected, TOF-SIMS gives component information based on bombardment of the sample with a focused primary ion beam. The penetrated ion transmits some of its energy to the lattice atoms, some of which move toward the surface and transfer energy to the surface ions for emission. This process is known as particle sputter-

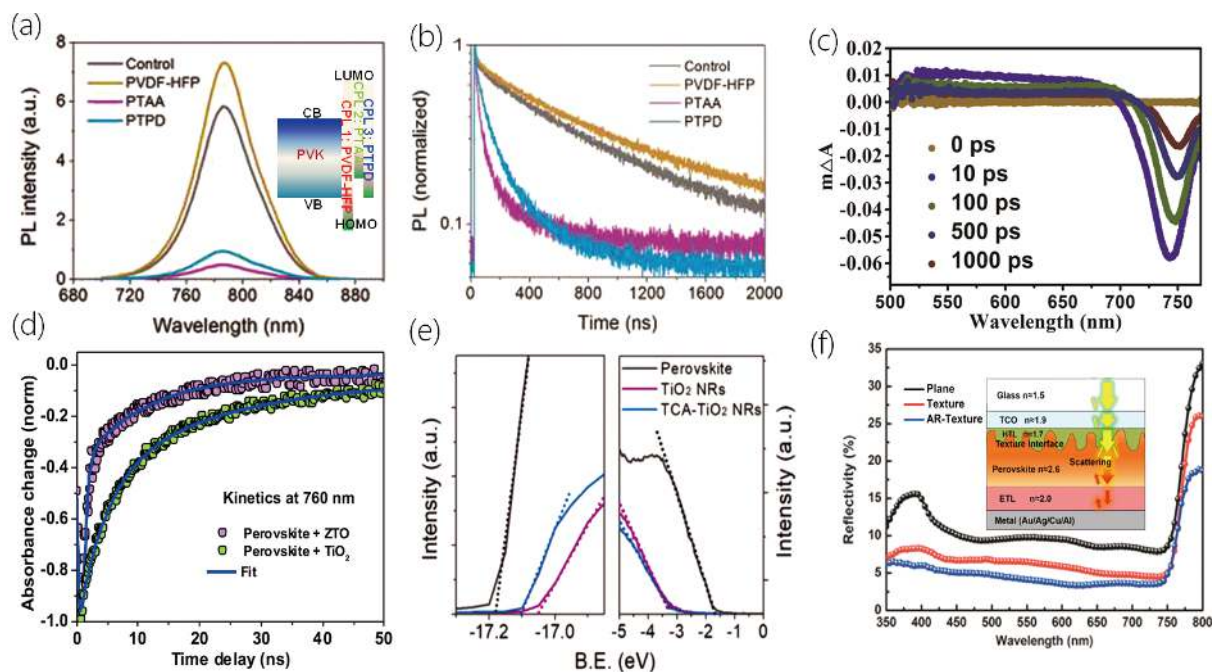


Fig. 4. (Color online) (a) Steady state and (b) time resolved photoluminescence (PL) spectra of perovskite films with different back contact layers. Reproduced with permission from Ref. [105]. Copyright 2018, Wiley. (c) Transmission ( $\Delta T/T$ ) spectra of devices. Reproduced with permission from Ref. [122]. Copyright 2020, ELSEVIER. (d) Transient absorption kinetics of perovskite films with different substrates. Reproduced with permission from Ref. [124]. Copyright 2015, ACS. (e) Ultraviolet photoelectron spectroscopy (UPS) spectra showing the energy-level alignment of the interfaces. Reproduced with permission from Ref. [125]. Copyright 2020, Wiley. (f) Reflectivity spectra of perovskite films on textured substrates. Reproduced with permission from Ref. [128]. Copyright 2019, ACS.

ing. Most of the sputtering particles are neutral atoms and molecules, while a small part are atoms, molecules, and molecular fragments with positive and negative charges. Ionized secondary particles (e.g., atoms, molecules, atomic groups, etc.) are separated by mass spectrometry according to the mass charge ratio, providing information about the compositional distribution of the elements in 3D. In this way, the location and component of interfaces could be measured through distribution of targeted marker elements or functional groups along the sputtering route. Other groups (e.g., halides, metal ions, etc.) that are commonly tracked during TOF-SIMS measurements can reveal the composition of interfaces and the diffusion/migration of metal elements or ions across the interfaces<sup>[100–102]</sup>. An illustration of the TOF-SIMS experiment on a thin-film device structure is presented in Figs. 3(f) and 3(g). By analyzing the HTL components of the device, especially the atomic and molecular A-site, Christians *et al.* used TOF-SIMS to assess the compositional changes in  $\text{TiO}_2/\text{FAMACs}/\text{HTM}/\text{Au}$  devices that had been under continuous operation for different times, discovering a dramatic composition change at the perovskite/HTM interface<sup>[103]</sup>. In addition, by using TOF-SIMS, not only the detailed components distribution in HTL but also the composition across the interface could be clearly demonstrated. This provides persuasive evidence for the existence of interfacial thin modifier<sup>[104]</sup>.

When considering TOF-SIMS, one's attention should be paid to the choice of tracking makers because some markers like benzene rings are not easy to detect. For example, when proving the existence of surface ultrathin modifiers, we found TOF-SIMS had difficulties in detecting characteristic group of benzene ring in molecules such as Spiro-OMeTAD or polyTPD, while the fluorine atom instead can be easily

tracked<sup>[105]</sup>. Using this detectable marker, we found that the polymer additives introduced via antisolvent dripping mostly located near the back surface/interface of perovskite film, playing a role of interfacial passivation.

### 3.2. Optical characterization

From this analysis, it can be seen that the morphology and component of the junction/interface part could be directly investigated by some professional measurements. However, it is not that easy to directly investigate the optoelectronic properties of the interfaces themselves. Optical characterization on the stacked layers usually aims at the influence of the interfaces on the physical properties of an adjacent perovskite layer. In this part, we show some optical characterizations that can reflect the role of interfaces.

PL, including steady state and time resolved PL (TRPL) spectra, is a commonly used method. Typically, PL characterization on perovskite films with buffer layers (contain heterojunction interfaces) can demonstrate the influence of interfaces, crystallization quality (defect density) of the entire perovskite film or the contact region. Buffer layer-induced contact passivation or enhanced crystallization (that means less defect states or grain boundaries) usually enables an enhanced PL intensity and elongated PL lifetime, while a blue shift of the peak is indicative of the decrease in spontaneous nonradiative recombination from the trap states<sup>[106–110]</sup>. However, when a conducting or semiconducting buffer layer and the perovskite film form an electrical contact with type-II energy-level alignment at the interface (Fig. 4(a)), it usually leads to quenched PL intensity and decreased PL lifetime of perovskite (Fig. 4(b)), which is mainly due to efficient and fast charges transfer and electron-hole separation via the interface<sup>[105, 111, 112]</sup>.

In our opinion, if a charge (either holes or electrons) acceptor buffer layer with passivative surface is adopted to form contact with perovskite, then one should pay special attention to the conclusion made from PL and TRPL results because both passivation effect (cause enlarged PL intensity and TRPL lifetime) and charge transfer effect (cause decreased PL intensity and TRPL lifetime) exist in this contact<sup>[113–115]</sup>. For example, when developing a passivative intermediate layer at the ETL/perovskite or HTL/perovskite interface, the PL intensity and TRPL lifetime of perovskite on buffer layer would be either enhanced or suppressed, depending on the competition between passivation induced PL enhancement and ETL/HTL induced PL quenching. Therefore, more persuasive comparison experiments should be provided to classify the separate role that each has played<sup>[105]</sup>.

Besides the photoluminescence spectrum, transient absorption spectroscopy (TAS) is a powerful technique that allows studying carrier dynamics both in bulk film and at interfaces. The change in light absorption or reflection is recorded by adjusting the time interval between the pump pulse and the probe pulse arriving at the sample. In addition, TAS provides indirect information on contact interfaces by measuring the absorption behaviors of perovskite film itself<sup>[116–121]</sup>. Analysis on ground state bleaching could reflect the intrinsic properties of perovskite (e.g., bandgap, composition, etc.). For example, when using TAS to research OA passivated perovskite films, the OA-modified film witnessed a more rapidly decreased signal compared to its original GSB peak, as well as the control counterpart (Fig. 4(c))<sup>[122]</sup>. Another important role that TAS plays is to evaluate the charge extraction at the heterojunction<sup>[123]</sup>. By using ultrafast transient absorption measurement, Bera *et al.* found that mesoporous Zn<sub>2</sub>SnO<sub>4</sub> could serve as efficient electron transporting material that enabled efficient charge extraction at the Zn<sub>2</sub>SnO<sub>4</sub>/perovskite interface (Fig. 4(d)); while solar cells with Zn<sub>2</sub>SnO<sub>4</sub> exhibit negligible electrical hysteresis and exceptionally high stability<sup>[124]</sup>.

For the interface contact for solar cell application, energy-level alignments at the interface play a critical role in charge dynamics. An ultraviolet photoelectron spectrometer (UPS) is frequently used to evaluate this key parameter. Because the energy of UV excitation light source is low, it can only ionize the valence electrons and valence band electrons in the outer electronic orbit of atoms, and can distinguish the vibrational energy levels of molecules. The penetration/detection depth during UPS measurement is as small as several (typically within 5 nm) nanometers. Therefore, to uncover the band alignment at the interface of two layers, one needs to carry out separate UPS measurement on each layer (Fig. 4(e))<sup>[125]</sup>. It should be noted that characterization on each free layer does not ensure an accurate description of the real interfacial energy alignment if there is a functional connection between the two layers. Consequently, in-situ direct characterization of the energy-level alignment at the deeply buried interface is an appealing challenge that is yet to be researched.

To enhance optical properties of perovskite films, effective light management is useful for increasing light absorption. An artificial structure with textured surface was thus developed to form contact with perovskite film<sup>[126]</sup>. With light scattering at the interface, enhanced light absorption or

decreased light transmittance loss can be achieved. Therefore, a common method such as absorption or transmittance spectra, even though it is an indirect way for interface characterization, is typically useful to evaluate these artificial nanostructured interfaces<sup>[127]</sup>. Xu *et al.* showed that the purposely fabricated PTAA/perovskite textured interface helped to reduce optical loss and benefited the band edge absorption of MAPbI<sub>3</sub> film, leading to increased EQE and the photocurrent (Fig. 4(f))<sup>[128]</sup>. Light absorption and transmittance spectra, better with optical simulations, have contributed considerably in correlated works with interfacial structure design, as well as tandem structures<sup>[129, 130]</sup>.

### 3.3. Electrical characterization

As optoelectronic devices, perovskite solar cells mainly work on charge transfer and extraction at interfaces. Electrical characterization on these processes is of great importance. Compared to the main indirect optical measurements, electrical characterization on perovskite layers with heterojunction interfaces have proven to be more straightforward to get information of interfaces. In this part, we analyze some typical electrical methods that can directly reflect the properties of interfacial contact.

Transient photocurrent (TPC) characterization is a typical process to depict the charge transfer extraction at the perovskite interfaces. In a short circuit condition, the largest photocurrent output will drop after the transient light excitation disappears. The faster the photocurrent drops, the faster and more efficient the charges transfer extraction will be<sup>[131–133]</sup>. Therefore, we can see from the reported literature that when an efficient ETL or HTL is adopted to form electrical contact with perovskite, the photocurrent decay is usually much faster compared to that for the inefficient ones<sup>[134]</sup>. We have used TPC to show that an energy-level alignment with flattened band offset between the valence band of perovskite and the highest occupied molecular orbit (HOMO) of the HTL layer benefited charge extraction at the interface (Fig. 5(a))<sup>[105]</sup>.

In the open circuit condition, however, the neat photocurrent output is zero due to complete charge recombination—either via intrinsic electron/hole recombination or via trap state induced nonradiative recombination. In this model, photovoltage is usually tracked to evaluate the interfacial charge recombination because defect induced charge nonradiative recombination is much faster than the intrinsic recombination<sup>[135–139]</sup>. Transient photovoltage (TPV) characterization is accordingly used when investigating interfacial charge recombination (Fig. 5(b)). Tan *et al.* showed that interfacial contact by passivative Cl coordination on perovskite can efficiently suppress nonradiative recombination, leading to an elongated photovoltage decay lifetime<sup>[60]</sup>.

Electrochemical impedance spectrum (EIS) a similar characterization that can also reflect the interfacial charge dynamics at open circuit conditions. By varying the bias voltage applied on the perovskite solar cells, different charge behaviors can be modulated. EIS measurements are commonly adopted in dye-sensitized solar cells to show three distinct charge processes in the solar cells: charge collection by electrode (the fastest, high frequency), the interfacial charge transfer between sensitizer dye and nanoparticles (TiO<sub>2</sub>) (the modest, middle frequency), and charge transport in the liquid electro-



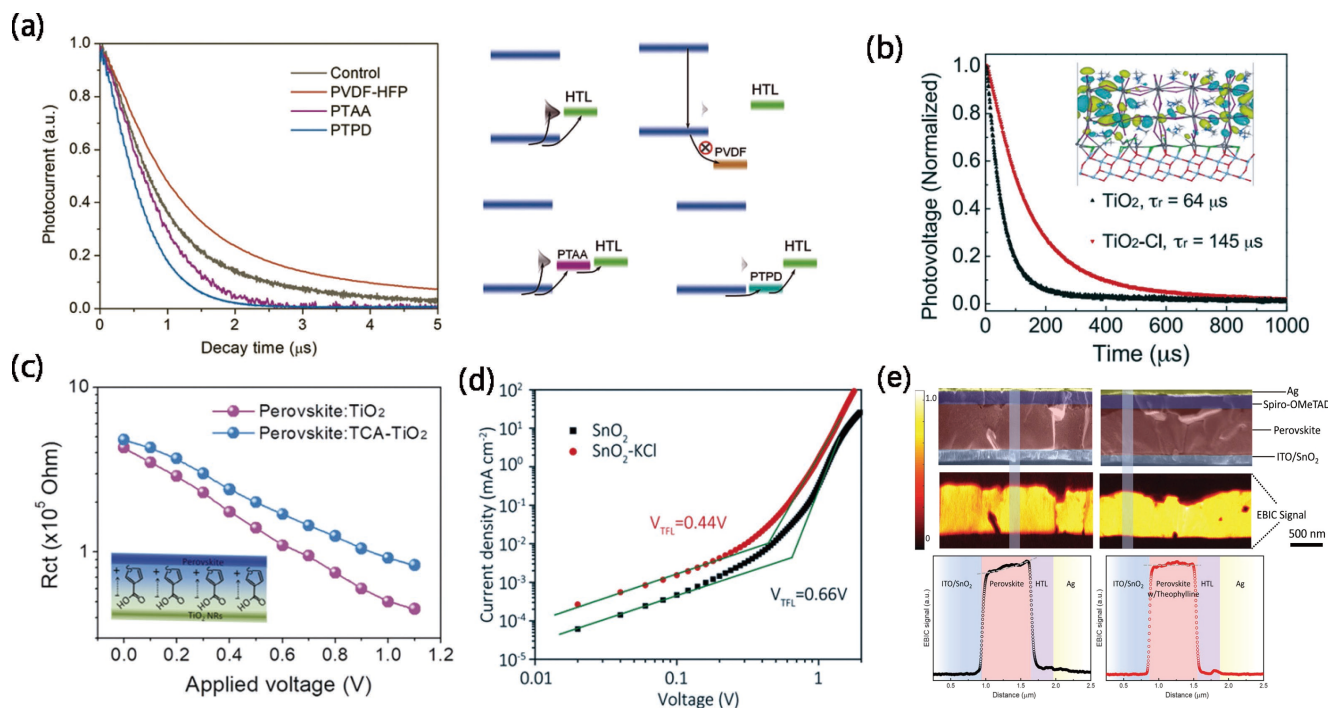


Fig. 5. (Color online) (a) Transient photocurrent spectra of perovskite films with different contact thin layers. Reproduced with permission from Ref. [105]. Copyright 2019, Wiley. The energy-level alignments at interface are also given for comparison. Reproduced with permission from Ref. [134]. Copyright 2019, Wiley. (b) Transient photovoltage spectra of perovskite films with different  $\text{TiO}_2$  ETL. The inset shows the contact passivation of perovskite by interfacial Cl. Reproduced with permission from Ref. [60]. Copyright 2017, Science. (c) Charge transfer recombination resistance at different bias voltages in electrochemical impedance spectrum measurement. Reproduced with permission from Ref. [146]. Copyright 2020, Wiley. (d) Space-charge-limited current (SCLC) characterization of perovskite solar cells with different  $\text{SnO}_2$  ETLs. Reproduced with permission from Ref. [153]. Copyright 2020, Wiley. (e) Electron beam induced current (EBIC) measurement of the current mapping at cross-section interfaces. Reproduced with permission from Ref. [160]. Copyright 2019, Science.

lyte (the slowest, low frequency)<sup>[140–143]</sup>. However, in solid state perovskite solar cells, distinguishing these three processes is difficult because they are similarly efficient. So, we usually observed one EIS arc response that is mainly located at middle frequency range (1–100 kHz)<sup>[144, 145]</sup>. In this way, a charge transfer recombination resistance ( $R_{ct}$ ) at the open circuit voltage could demonstrate charge recombination loss at the interface, with a larger  $R_{ct}$  value showing a depressed charge recombination from defects (Fig. 5(c))<sup>[146]</sup>. Because interfaces in perovskite solar cells had effect of charge accumulation, EIS characterization of this device under illumination conditions demonstrated a giant capacitance at the low-frequency domain, which is indicative of the accumulation of carriers at the interfaces<sup>[125]</sup>.

We have noted that, regarding the two typical charge behaviors (i.e., charge transfer separation/extraction and charge transfer recombination), the corresponding electrical characterization has mainly been carried out at either short circuit condition (charge transfer separation/extraction) or open circuit condition (charge transfer recombination). Considering that the electrochemical impedance at zero bias is usually too large to be regularly and precisely determined, some important interfacial information relating to charge transfer extraction might have been ignored in the previous literature. This speculation is yet to be uncovered.

As a facile  $I$ - $V$  measurement, space-charge-limited current (SCLC) characterization has usually been adopted to evaluate some new HTLs or ETLs that can enable interfacial passivation except for its basic charge acceptor role<sup>[147–150]</sup>. More

traps at this region would need a larger voltage to get them fulfilled by charges. In this case, a small trap-filled limited voltage ( $V_{TFL}$ ) means a less trap density at the interface. The trap density  $N_t$  is calculated from equation  $V_{TFL} = eN_tL^2/2\epsilon\epsilon_0$ , where  $e$  is the elementary charge,  $L$  is the thickness of perovskite film,  $\epsilon$  is the relative dielectric constant,  $\epsilon_0$  is the vacuum permittivity, and  $V_{TFL}$  is the trap-filling limit voltage<sup>[151]</sup>. Using the SCLC method (Fig. 5(d)), Zhu *et al.* also showed that a composite KCl- $\text{SnO}_2$  buffer layer as ETL is useful to simultaneously passivate the defects at the ETL/perovskite interface and the grain boundaries of perovskite film<sup>[152]</sup>.

Considering that the organic/inorganic hybrid perovskite materials is volatile and decomposable under exposure to strong optical, thermal, electrical or humidity stimulation, the optical and electrical measurements mentioned here have not contained very strong optical radiation or large electric fields. However, some characterization with very high space resolution ratio (which usually needs a focused stimulation source, such as an electron beam) can provide detailed measurements on precisely targeted interfaces. The electron beam induced current (EBIC) process was developed to measure the current mapping of cross-section including interfaces because we know that electron beam from sources like SEM chamber has high space resolution ratio<sup>[153–159]</sup>. From this EBIC mapping, charge generation largely happened at both ETL/perovskite and HTL/perovskite interfaces<sup>[155]</sup>. Furthermore, the detailed difference in charge dynamics at the two interfaces could be evaluated by comparing the two EBIC signals, which are closely correlated with defect induced charge

recombination. Using interface engineering (e.g., passivator treatment), an enlarged hole diffusion length was shown to be obtained together with a balanced hole-electron collection<sup>[160]</sup>, as demonstrated from decreased EBIC difference between the two interfaces (Fig. 5(e)). Consequently, EBIC is an attractive in direct evaluation on interfaces engineering. However, in this process, one should always keep in mind that a large dose exposure or strong stimulation of volatile perovskite would induce a composition change that would risk the repeatability and persuasion of the characterization results. Therefore, other precisely localized measurements but with a gentler process should be developed.

#### 4. Challenges and outlook

Interface modulation has played an increasingly important role in performance improvement and commercialization of perovskite solar cells, in which characterization of this critical component should be fully and persuasively developed. Our analysis of the presently reported interface-related techniques allows us to summarize several detailed problems that should be given attention when carrying out measurements on interfaces.

It was found that some interface-related conclusions were not persuasive based on inadequate characterizations. A typical example is the PL and TRPL research of the perovskite/buffer layer heterojunction, where improved charge transfer and contact passivation coexist. Additional experiments are needed to make two distinct effects clear: charge transfer caused a decrease in PL intensity and TRPL lifetime, and passivation induced enhancement in these two factors. Some characterization methods (e.g., electrochemical impedance spectrum) originated from other photovoltaic techniques. Therefore, their direct adoption for solid state perovskite thin-film solar cells might cause confusion when analyzing detailed charge dynamics at interfaces because there is no remarkable difference in the speed (frequency) of charge transfer and transport at different parts of a perovskite solar cell. A precise and stable impedance equipment with high time resolution is required to tell different kinetics apart.

Considering the intrinsic chemical and phase stability of perovskite, another challenge is to keep the perovskite phase as it is during various measurement conditions. Usually, perovskite samples would be tested in ambient air with a certain humidity and oxygen that will deteriorate the chemical and phase stability of perovskite materials. Optoelectronic measurements under intense light, high temperature or large electric field would also cause degradation, iron migration or phase variation in perovskite, which would influence the accuracy of measurement results correlated with interfaces.

A direct and more reliable characterization strategy is required to better serve the working mechanism of interface-related modulation. Simultaneous measurements on in-situ morphology together with intrinsic optoelectronic properties seem attractive in revealing interfacial species behaviors at a precise location. This might also require a robust sample preparation process that should present the real interface part while keeping its original properties. In addition, this research field would benefit more from a deeper study on how to characterize some interesting dynamical process when a

solar cell is under work, such as electron transfer induced potential variation, field induced trap filling, or even light scattering by nanostructured interfaces.

#### 5. Conclusions

Interface-related characterization techniques have played a major role in understanding the physical and chemical properties and evolution of PSCs. In this review, we have illustrated the importance of interface-characterization methods for PSC research. These techniques allow us to obtain insights of the nano- and microscale details of perovskite surfaces and interfaces. While some characterization techniques indeed provide insightful understanding of the interfaces, new strategic and reliable methods are still needed. This requires a thorough and full understanding of the nature of the interfaces, such as composition, morphology, defects, and stability. We have no doubt that these versatile tools will continue to enable the exploration of questions related to the micro and nano structures in PSCs, bringing these materials beyond the state-of-the-art.

#### Acknowledgements

This publication is based in part on the work supported by the Science and Technology Development Project of Henan Province (grant no. 202300410048), the Intelligence Introduction Plan of Henan Province in 2021 (CXJD2021008), the Postdoctoral Fund of China (grant no. FJ3050A0670111), the Henan University Fund, and the Canada Research Chairs Supplement Fund and New Frontiers in Research Fund (NFRF).

#### References

- [1] Dullweber T, Stöhr M, Kruse C, et al. Evolutionary PERC+ solar cell efficiency projection towards 24% evaluating shadow-mask-deposited poly-Si fingers below the Ag front contact as next improvement step. *Sol Energy Mater Sol Cells*, 2020, 212, 110586
- [2] Yu J, Liao M D, Yan D, et al. Activating and optimizing evaporation-processed magnesium oxide passivating contact for silicon solar cells. *Nano Energy*, 2019, 62, 181
- [3] Allen T G, Bullock J, Yang X B, et al. Passivating contacts for crystalline silicon solar cells. *Nat Energy*, 2019, 4, 914
- [4] Yoshikawa K, Kawasaki H, Yoshida W, et al. Silicon heterojunction solar cell with interdigitated back contacts for a photoconversion efficiency over 26%. *Nat Energy*, 2017, 2, 1
- [5] Kato T, Wu J L, Hirai Y, et al. Record efficiency for thin-film polycrystalline solar cells up to 22.9% achieved by Cs-treated Cu(In, Ga)(Se, S)<sub>2</sub>. *IEEE J Photovolt*, 2019, 9, 325
- [6] Metzger W K, Grover S, Lu D, et al. Exceeding 20% efficiency with *in situ* group V doping in polycrystalline CdTe solar cells. *Nat Energy*, 2019, 4, 837
- [7] Burst J M, Duenow J N, Albin D S, et al. CdTe solar cells with open-circuit voltage breaking the 1 V barrier. *Nat Energy*, 2016, 1, 16015
- [8] Green M A, Hishikawa Y, Dunlop E D, et al. Solar cell efficiency tables (Version 53). *Prog Photovolt: Res Appl*, 2019, 27, 3
- [9] Jeong M, Choi I W, Go E M, et al. Stable perovskite solar cells with efficiency exceeding 24.8% and 0.3-V voltage loss. *Science*, 2020, 369, 1615
- [10] Han T H, Tan S, Xue J J, et al. Interface and defect engineering for metal halide perovskite optoelectronic devices. *Adv Mater*, 2019, 31, 1803515
- [11] Bai Y, Meng X Y, Yang S H. Interface engineering for highly effi-



- cient and stable planar p-i-n perovskite solar cells. *Adv Energy Mater*, 2018, 8, 1701883
- [12] Schulz P, Cahen D, Kahn A. Halide perovskites: Is it all about the interfaces. *Chem Rev*, 2019, 119, 3349
- [13] Zhang F, Zhu K. Additive engineering for efficient and stable perovskite solar cells. *Adv Energy Mater*, 2020, 10, 1902579
- [14] Zuo C T, Bolink H J, Han H W, et al. Advances in perovskite solar cells. *Adv Sci*, 2016, 3, 1500324
- [15] Jeon N J, Na H, Jung E H, et al. A fluorene-terminated hole-transporting material for highly efficient and stable perovskite solar cells. *Nat Energy*, 2018, 3, 682
- [16] Jiang Q, Zhao Y, Zhang X W, et al. Surface passivation of perovskite film for efficient solar cells. *Nat Photonics*, 2019, 13, 460
- [17] Yang G, Ren Z W, Liu K, et al. Stable and low-photovoltage-loss perovskite solar cells by multifunctional passivation. *Nat Photonics*, 2021, 15, 681
- [18] Shao S Y, Loi M A. The role of the interfaces in perovskite solar cells. *Adv Mater Interfaces*, 2020, 7, 1901469
- [19] Miao Y W, Zheng M M, Wang H X, et al. *In-situ* secondary annealing treatment assisted effective surface passivation of shallow defects for efficient perovskite solar cells. *J Power Sources*, 2021, 492, 229621
- [20] Wang P, Cai F, Yang L, et al. Eliminating light-soaking instability in planar heterojunction perovskite solar cells by interfacial modifications. *ACS Appl Mater Interfaces*, 2018, 10, 33144
- [21] Zheng F, Wen X M, Bu T L, et al. Slow response of carrier dynamics in perovskite interface upon illumination. *ACS Appl Mater Interfaces*, 2018, 10, 31452
- [22] Chen W, Zhou Y C, Chen G C, et al. Alkali chlorides for the suppression of the interfacial recombination in inverted planar perovskite solar cells. *Adv Energy Mater*, 2019, 9, 1803872
- [23] Xiong S B, Hao T, Sun Y Y, et al. Defect passivation by nontoxic biomaterial yields 21% efficiency perovskite solar cells. *J Energy Chem*, 2021, 55, 265
- [24] Sherkar T S, Momblona C, Gil-Escrig L, et al. Recombination in perovskite solar cells: Significance of grain boundaries, interface traps, and defect ions. *ACS Energy Lett*, 2017, 2, 1214
- [25] Leguy A M A, Hu Y H, Campoy-Quiles M, et al. Reversible hydration of  $\text{CH}_3\text{NH}_3\text{PbI}_3$  in films, single crystals, and solar cells. *Chem Mater*, 2015, 27, 3397
- [26] Deng F, Li X T, Lv X, et al. Low-temperature processing all-inorganic carbon-based perovskite solar cells up to 11.78% efficiency via alkali hydroxides interfacial engineering. *ACS Appl Energy Mater*, 2020, 3, 401
- [27] Wu J H, Shi J J, Li Y M, et al. Quantifying the interface defect for the stability origin of perovskite solar cells. *Adv Energy Mater*, 2019, 9, 1901352
- [28] Wu T T, Zhen C, Zhu H Z, et al. Gradient Sn-doped heteroepitaxial film of faceted rutile  $\text{TiO}_2$  as an electron selective layer for efficient perovskite solar cells. *ACS Appl Mater Interfaces*, 2019, 11, 19638
- [29] Wang G X, Wang L P, Qiu J H, et al. *In situ* passivation on rear perovskite interface for efficient and stable perovskite solar cells. *ACS Appl Mater Interfaces*, 2020, 12, 7690
- [30] Hsieh H C, Hsiow C Y, Lin K F, et al. Analysis of defects and traps in N-I-P layered-structure of perovskite solar cells by charge-based deep level transient spectroscopy (Q-DLTS). *J Phys Chem C*, 2018, 122, 17601
- [31] Liu Z H, Qiu L B, Ono L K, et al. A holistic approach to interface stabilization for efficient perovskite solar modules with over 2,000-hour operational stability. *Nat Energy*, 2020, 5, 596
- [32] Mahapatra A, Prochowicz D, Tavakoli M M, et al. A review of aspects of additive engineering in perovskite solar cells. *J Mater Chem A*, 2020, 8, 27
- [33] Cao S L, Wang H X, Li H Y, et al. Critical role of interface contact modulation in realizing low-temperature fabrication of efficient and stable  $\text{CsPbI}_2\text{Br}_2$  perovskite solar cells. *Chem Eng J*, 2020, 394, 124903
- [34] Tavakoli M M, Tavakoli R, Yadav P, et al. A graphene/ZnO electron transfer layer together with perovskite passivation enables highly efficient and stable perovskite solar cells. *J Mater Chem A*, 2019, 7, 679
- [35] Zheng X P, Hou Y, Bao C X, et al. Managing grains and interfaces via ligand anchoring enables 22.3%-efficiency inverted perovskite solar cells. *Nat Energy*, 2020, 5, 131
- [36] Wu Z F, Liu Z H, Hu Z H, et al. Highly efficient and stable perovskite solar cells via modification of energy levels at the perovskite/carbon electrode interface. *Adv Mater*, 2019, 31, 1804284
- [37] Tavakoli M M, Saliba M, Yadav P, et al. Synergistic crystal and interface engineering for efficient and stable perovskite photovoltaics. *Adv Energy Mater*, 2019, 9, 1802646
- [38] Yoo J J, Wiegbold S, Sponseller M C, et al. An interface stabilized perovskite solar cell with high stabilized efficiency and low voltage loss. *Energy Environ Sci*, 2019, 12, 2192
- [39] Boyd C C, Checharoen R, Leijtens T, et al. Understanding degradation mechanisms and improving stability of perovskite photovoltaics. *Chem Rev*, 2019, 119, 3418
- [40] Pearson A J, Eperon G E, Hopkinson P E, et al. Oxygen degradation in mesoporous  $\text{Al}_2\text{O}_3/\text{CH}_3\text{NH}_3\text{PbI}_{3-x}\text{Cl}_x$  perovskite solar cells: Kinetics and mechanisms. *Adv Energy Mater*, 2016, 6, 1600014
- [41] Noel N K, Stranks S D, Abate A, et al. Lead-free organic-inorganic tin halide perovskites for photovoltaic applications. *Energy Environ Sci*, 2014, 7, 3061
- [42] Seo J Y, Kim H S, Akin S, et al. Novel p-dopant toward highly efficient and stable perovskite solar cells. *Energy Environ Sci*, 2018, 11, 2985
- [43] Chen J Z, Park N G. Inorganic hole transporting materials for stable and high efficiency perovskite solar cells. *J Phys Chem C*, 2018, 122, 14039
- [44] Berhe T A, Su W N, Chen C H, et al. Organometal halide perovskite solar cells: Degradation and stability. *Energy Environ Sci*, 2016, 9, 323
- [45] Niu G D, Guo X D, Wang L D. Review of recent progress in chemical stability of perovskite solar cells. *J Mater Chem A*, 2015, 3, 8970
- [46] Niu T Q, Lu J, Munir R, et al. Stable high-performance perovskite solar cells via grain boundary passivation. *Adv Mater*, 2018, 30, 1706576
- [47] Guo Q, Yuan F, Zhang B, et al. Passivation of the grain boundaries of  $\text{CH}_3\text{NH}_3\text{PbI}_3$  using carbon quantum dots for highly efficient perovskite solar cells with excellent environmental stability. *Nanoscale*, 2018, 11, 115
- [48] Yang J, Siempelkamp B D, Liu D, et al. Investigation of  $\text{CH}_3\text{NH}_3\text{PbI}_3$  degradation rates and mechanisms in controlled humidity environments using *in situ* techniques. *ACS Nano*, 2015, 9, 1955
- [49] Song Z N, Abate A, Wathage S C, et al. Perovskite solar cell stability in humid air: Partially reversible phase transitions in the  $\text{PbI}_2\text{-CH}_3\text{NH}_3\text{I-H}_2\text{O}$  system. *Adv Energy Mater*, 2016, 6, 1600846
- [50] Niu G D, Li W Z, Meng F Q, et al. Study on the stability of  $\text{CH}_3\text{NH}_3\text{PbI}_3$  films and the effect of post-modification by aluminum oxide in all-solid-state hybrid solar cells. *J Mater Chem A*, 2014, 2, 705
- [51] Chen Y, Li N, Wang L, et al. Impacts of alkaline on the defects property and crystallization kinetics in perovskite solar cells. *Nat Commun*, 2019, 10, 1112
- [52] Zheng L L, Chung Y H, Ma Y Z, et al. A hydrophobic hole transporting oligothiophene for planar perovskite solar cells with improved stability. *Chem Commun*, 2014, 50, 11196
- [53] Li X D, Ke S Z, Feng X X, et al. Enhancing the stability of per-

- ovskite solar cells through cross-linkable and hydrogen bonding multifunctional additives. *J Mater Chem A*, 2021, 9, 12684
- [54] Yang J, Liu C, Cai C S, et al. High-performance perovskite solar cells with excellent humidity and thermo-stability via fluorinated perylene diimide. *Adv Energy Mater*, 2019, 9, 1900198
- [55] Wu W Q, Yang Z, Rudd P N, et al. Bilateral alkylamine for suppressing charge recombination and improving stability in blade-coated perovskite solar cells. *Sci Adv*, 2019, 5, eaav8925
- [56] Zheng X P, Troughton J, Gasparini N, et al. Quantum dots supply bulk- and surface-passivation agents for efficient and stable perovskite solar cells. *Joule*, 2019, 3, 1963
- [57] Yu B, Zuo C, Shi J, et al. Defect engineering on all-inorganic perovskite solar cells for high efficiency. *J Semicond*, 2021, 42, 050203
- [58] Cheng M, Zuo C, Wu Y, et al. Charge-transport layer engineering in perovskite solar cells. *Sci Bull*, 2020, 65, 1237
- [59] Zhang J, Hou S X, Li R J, et al. I/P interface modification for stable and efficient perovskite solar cells. *J Semicond*, 2020, 41, 052202
- [60] Tan H, Jain A, Voznyy O, et al. Efficient and stable solution-processed planar perovskite solar cells via contact passivation. *Science*, 2017, 355, 722
- [61] Tan W L, Choo Y Y, Huang W C, et al. Oriented attachment as the mechanism for microstructure evolution in chloride-derived hybrid perovskite thin films. *ACS Appl Mater Interfaces*, 2019, 11, 39930
- [62] Ren J, Luo Q, Hou Q Z, et al. Suppressing charge recombination and ultraviolet light degradation of perovskite solar cells using silicon oxide passivation. *ChemElectroChem*, 2019, 6, 3167
- [63] Ha J, Kim H, Lee H, et al. Device architecture for efficient, low-hysteresis flexible perovskite solar cells: Replacing TiO<sub>2</sub> with C60 assisted by polyethylenimine ethoxylated interfacial layers. *Sol Energy Mater Sol Cells*, 2017, 161, 338
- [64] Zhang X, Ma S, You J B, et al. Tailoring molecular termination for thermally stable perovskite solar cells. *J Semicond*, 2021, 42, 112201
- [65] Shin S S, Suk J H, Kang B J, et al. Energy-level engineering of the electron transporting layer for improving open-circuit voltage in dye and perovskite-based solar cells. *Energy Environ Sci*, 2019, 12, 958
- [66] Idrissi S, Ziti S, Labrim H, et al. Band gaps of the solar perovskites photovoltaic CsXCl<sub>3</sub> (X = Sn, Pb or Ge). *Mater Sci Semicond Process*, 2021, 122, 105484
- [67] Zhang L H, Zhang X, Lu G. Band alignment in two-dimensional halide perovskite heterostructures: Type I or type II. *J Phys Chem Lett*, 2020, 11, 2910
- [68] Liao C S, Yu Z L, He P B, et al. Effects of composition modulation on the type of band alignments for Pd<sub>2</sub>Se<sub>3</sub>/CsSnBr<sub>3</sub> van der Waals heterostructure: A transition from type I to type II. *J Power Sources*, 2020, 478, 229078
- [69] Raoui Y, Ez-Zahraouy H, Kazim S, et al. Energy level engineering of charge selective contact and halide perovskite by modulating band offset: Mechanistic insights. *J Energy Chem*, 2021, 54, 822
- [70] Lim K G, Ahn S, Kim Y H, et al. Universal energy level tailoring of self-organized hole extraction layers in organic solar cells and organic-inorganic hybrid perovskite solar cells. *Energy Environ Sci*, 2016, 9, 932
- [71] Begum R, Parida M R, Abdelhady A L, et al. Engineering interfacial charge transfer in CsPbBr<sub>3</sub> perovskite nanocrystals by heterovalent doping. *J Am Chem Soc*, 2017, 139, 731
- [72] Meggiolaro D, Mosconi E, Proppe A H, et al. Energy level tuning at the MAPbI<sub>3</sub> perovskite/contact interface using chemical treatment. *ACS Energy Lett*, 2019, 4, 2181
- [73] Choi H, Jeong J, Kim H B, et al. Cesium-doped methylammonium lead iodide perovskite light absorber for hybrid solar cells. *Nano Energy*, 2014, 7, 80
- [74] Du K Z, Wang X M, Han Q W, et al. Heterovalent B-site co-alloying approach for halide perovskite bandgap engineering. *ACS Energy Lett*, 2017, 2, 2486
- [75] Unger E L, Kegelmann L, Suchan K, et al. Roadmap and roadblocks for the band gap tunability of metal halide perovskites. *J Mater Chem A*, 2017, 5, 11401
- [76] Ding X D, Wang H X, Chen C, et al. Passivation functionalized phenothiazine-based hole transport material for highly efficient perovskite solar cell with efficiency exceeding 22%. *Chem Eng J*, 2021, 410, 128328
- [77] Xie L S, Cao Z Y, Wang J W, et al. Improving energy level alignment by adenine for efficient and stable perovskite solar cells. *Nano Energy*, 2020, 74, 104846
- [78] Zhang Z H, Li J, Fang Z M, et al. Adjusting energy level alignment between HTL and CsPbI<sub>2</sub>Br to improve solar cell efficiency. *J Semicond*, 2021, 42, 030501
- [79] Cao Q, Li Z, Han J, et al. Electron transport bilayer with cascade energy alignment for efficient perovskite solar cells. *Sol RRL*, 2019, 3, 1900333
- [80] Schulz P, Edri E, Kirmayer S, et al. Interface energetics in organometal halide perovskite-based photovoltaic cells. *Energy Environ Sci*, 2014, 7, 1377
- [81] Guo X, McCleese C, Kolodziej C, et al. Identification and characterization of the intermediate phase in hybrid organic-inorganic MAPbI<sub>3</sub> perovskite. *Dalton Trans*, 2016, 45, 3806
- [82] Shkir M, Khan M T, AlFaify S. Novel Nd-doping effect on structural, morphological, optical, and electrical properties of facily fabricated PbI<sub>2</sub> thin films applicable to optoelectronic devices. *Appl Nanosci*, 2019, 9, 1417
- [83] Yang L, Wang X, Mai X, et al. Constructing efficient mixed-ion perovskite solar cells based on TiO<sub>2</sub> nanorod array. *J Colloid Interface Sci*, 2019, 534, 459
- [84] Chen Y, Meng Q, Xiao Y, et al. Mechanism of PbI<sub>2</sub> *in situ* passivated perovskite films for enhancing the performance of perovskite solar cells. *ACS Appl Mater Interfaces*, 2019, 11, 44101
- [85] Cui Q, Zhao X C, Lin H, et al. Improved efficient perovskite solar cells based on Ta-doped TiO<sub>2</sub> nanorod arrays. *Nanoscale*, 2017, 9, 18897
- [86] Liu J M, Zhu L Q, Xiang S S, et al. Cs-doped TiO<sub>2</sub> nanorod array enhances electron injection and transport in carbon-based CsPbI<sub>3</sub> perovskite solar cells. *ACS Sustain Chem Eng*, 2019, 7, 16927
- [87] Wu S F, Chen C, Wang J M, et al. Controllable preparation of rutile TiO<sub>2</sub> nanorod array for enhanced photovoltaic performance of perovskite solar cells. *ACS Appl Energy Mater*, 2018, 1, 1649
- [88] Chandrasekhar P S, Dubey A, Qiao Q Q. High efficiency perovskite solar cells using nitrogen-doped graphene/ZnO nanorod composite as an electron transport layer. *Sol Energy*, 2020, 197, 78
- [89] Zhao Y, Tan H, Yuan H, et al. Perovskite seeding growth of formamidinium-lead-iodide-based perovskites for efficient and stable solar cells. *Nat Commun*, 2018, 9, 1607
- [90] Nukunudompanich M, Budiutama G, Suzuki K, et al. Dominant effect of the grain size of the MAPbI<sub>3</sub> perovskite controlled by the surface roughness of TiO<sub>2</sub> on the performance of perovskite solar cells. *CrystEngComm*, 2020, 22, 2718
- [91] Jung E H, Jeon N J, Park E Y, et al. Efficient, stable and scalable perovskite solar cells using poly(3-hexylthiophene). *Nature*, 2019, 567, 511
- [92] Ravi V K, Santra P K, Joshi N, et al. Origin of the substitution mechanism for the binding of organic ligands on the surface of CsPbBr<sub>3</sub> perovskite nanocubes. *J Phys Chem Lett*, 2017, 8, 4988
- [93] Boyd C C, Shallcross R C, Moot T, et al. Overcoming redox reactions at perovskite-nickel oxide interfaces to boost voltages in perovskite solar cells. *Joule*, 2020, 4, 1759
- [94] Wu T H, Wang Y B, Li X, et al. Efficient defect passivation for perovskite solar cells by controlling the electron density distribu-

- tion of donor- $\pi$ -acceptor molecules. *Adv Energy Mater*, 2019, 9, 1803766
- [95] Matteocci F, Busby Y, Pireaux J J, et al. Interface and composition analysis on perovskite solar cells. *ACS Appl Mater Interfaces*, 2015, 7, 26176
- [96] Busby Y, Agresti A, Pescetelli S, et al. Aging effects in interface-engineered perovskite solar cells with 2D nanomaterials: A depth profile analysis. *Mater Today Energy*, 2018, 9, 1
- [97] Xu D, Hua X, Liu S C, et al. *In situ* and real-time ToF-SIMS analysis of light-induced chemical changes in perovskite  $\text{CH}_3\text{NH}_3\text{PbI}_3$ . *Chem Commun Camb Engl*, 2018, 54, 5434
- [98] Harvey S P, Li Z, Christians J A, et al. Probing perovskite inhomogeneity beyond the surface: TOF-SIMS analysis of halide perovskite photovoltaic devices. *ACS Appl Mater Interfaces*, 2018, 10, 28541
- [99] Harvey S P, Zhang F, Palmstrom A, et al. Mitigating measurement artifacts in TOF-SIMS analysis of perovskite solar cells. *ACS Appl Mater Interfaces*, 2019, 11, 30911
- [100] Lee M V, Raga S R, Kato Y, et al. Transamidation of dimethylformamide during alkylammonium lead triiodide film formation for perovskite solar cells. *J Mater Res*, 2017, 32, 45
- [101] Lin W C, Kovalsky A, Wang Y C, et al. Interpenetration of  $\text{CH}_3\text{NH}_3\text{PbI}_3$  and  $\text{TiO}_2$  improves perovskite solar cells while  $\text{TiO}_2$  expansion leads to degradation. *Phys Chem Chem Phys*, 2017, 19, 21407
- [102] Yang B, Keum J, Ovchinnikova O S, et al. Deciphering halogen competition in organometallic halide perovskite growth. *J Am Chem Soc*, 2016, 138, 5028
- [103] Christians J A, Schulz P, Tinkham J S, et al. Tailored interfaces of unencapsulated perovskite solar cells for >1,000 hour operational stability. *Nat Energy*, 2018, 3, 68
- [104] Kim J, Lee Y, Gil B, et al. A  $\text{Cu}_2\text{O}$ - $\text{CuSCN}$  nanocomposite as a hole-transport material of perovskite solar cells for enhanced carrier transport and suppressed interfacial degradation. *ACS Appl Energy Mater*, 2020, 3, 7572
- [105] Tan F R, Tan H R, Saidaminov M I, et al. *In situ* back-contact passivation improves photovoltage and fill factor in perovskite solar cells. *Adv Mater*, 2019, 31, 1807435
- [106] Baloch A B, Alharbi F H, Grancini G, et al. Analysis of photocarrier dynamics at interfaces in perovskite solar cells by time-resolved photoluminescence. *J Phys Chem C*, 2018, 122, 26805
- [107] Lv Y, Cai B, Wu Y H, et al. High performance perovskite solar cells using  $\text{TiO}_2$  nanospindles as ultrathin mesoporous layer. *J Energy Chem*, 2018, 27, 951
- [108] Guo D, Bartsaghi D, Wei H, et al. Photoluminescence from radiative surface states and excitons in methylammonium lead bromide perovskites. *J Phys Chem Lett*, 2017, 8, 4258
- [109] Zhu X J, Du M Y, Feng J S, et al. High-efficiency perovskite solar cells with imidazolium-based ionic liquid for surface passivation and charge transport. *Angew Chem*, 2021, 133, 4284
- [110] Yang C, Wang H, Miao Y, et al. Interfacial molecular doping and energy level alignment regulation for perovskite solar cells with efficiency exceeding 23%. *Am Chem Soc*, 2021, 6, 2690
- [111] Kuo M Y, Spitha N, Hautzinger M P, et al. Distinct carrier transport properties across horizontally vs vertically oriented heterostructures of 2D/3D perovskites. *J Am Chem Soc*, 2021, 143, 4969
- [112] Pu Y C, Fan H C, Liu T W, et al. Methylamine lead bromide perovskite/protonated graphitic carbon nitride nanocomposites: Interfacial charge carrier dynamics and photocatalysis. *J Mater Chem A*, 2017, 5, 25438
- [113] Nouri E, Mohammadi M R, Xu Z X, et al. Improvement of the photovoltaic parameters of perovskite solar cells using a reduced-graphene-oxide-modified titania layer and soluble copper phthalocyanine as a hole transporter. *Phys Chem Chem Phys*, 2018, 20, 2388
- [114] Ramos F J, Jutteau S, Posada J, et al. Highly efficient  $\text{MoO}_x$ -free semitransparent perovskite cell for 4 T tandem application improving the efficiency of commercially-available Al-BSF silicon. *Sci Rep*, 2018, 8, 16139
- [115] Zhang W H, Ding Y, Jiang Y, et al. Simultaneously enhanced  $J_{sc}$  and FF by employing two solution-processed interfacial layers for inverted planar perovskite solar cells. *RSC Adv*, 2017, 7, 39523
- [116] Montcada N F, Marín-Beloqui J M, Cambarau W, et al. Analysis of photoinduced carrier recombination kinetics in flat and mesoporous lead perovskite solar cells. *ACS Energy Lett*, 2017, 2, 182
- [117] Zhu L Z, Ye J J, Zhang X H, et al. Performance enhancement of perovskite solar cells using a La-doped  $\text{BaSnO}_3$  electron transport layer. *J Mater Chem A*, 2017, 5, 3675
- [118] Ye T, Xing J, Petrović M, et al. Temperature effect of the compact  $\text{TiO}_2$  layer in planar perovskite solar cells: An interfacial electrical, optical and carrier mobility study. *Sol Energy Mater Sol Cells*, 2017, 163, 242
- [119] Serpetzoglou E, Konidakis I, Kakavelakis G, et al. Improved carrier transport in perovskite solar cells probed by femtosecond transient absorption spectroscopy. *ACS Appl Mater Interfaces*, 2017, 9, 43910
- [120] Dar M I, Franckevičius M, Arora N, et al. High photovoltage in perovskite solar cells: New physical insights from the ultrafast transient absorption spectroscopy. *Chem Phys Lett*, 2017, 683, 211
- [121] Gao Y B, Wu Y J, Liu Y, et al. Interface and grain boundary passivation for efficient and stable perovskite solar cells: The effect of terminal groups in hydrophobic fused benzothiadiazole-based organic semiconductors. *Nanoscale Horizons*, 2020, 5, 1574
- [122] Wu W Q, Zhong J X, Liao J F, et al. Spontaneous surface/interface ligand-anchored functionalization for extremely high fill factor over 86% in perovskite solar cells. *Nano Energy*, 2020, 75, 104929
- [123] Ghosh D, Chaudhary D K, Ali M Y, et al. All-inorganic quantum dot assisted enhanced charge extraction across the interfaces of bulk organo-halide perovskites for efficient and stable pin-hole free perovskite solar cells. *Chem Sci*, 2019, 10, 9530
- [124] Bera A, Bera A, Sheikh A D, et al. Fast crystallization and improved stability of perovskite solar cells with  $\text{Zn}_2\text{SnO}_4$  electron transporting layer: Interface matters. *ACS Appl Mater Interfaces*, 2015, 7, 28404
- [125] Afroz M A, Aranda C A, Tailor N K, et al. Impedance spectroscopy for metal halide perovskite single crystals: Recent advances, challenges, and solutions. *ACS Energy Lett*, 2021, 6, 3275
- [126] Jäger K, Sutter J, Hammerschmidt M, et al. Prospects of light management in perovskite/silicon tandem solar cells. *Nanophotonics*, 2021, 10, 1991
- [127] Chen B, Yu Z J, Manzoor S, et al. Blade-coated perovskites on textured silicon for 26%-efficient monolithic perovskite/silicon tandem solar cells. *Joule*, 2020, 4, 850
- [128] Xu C Y, Hu W, Wang G, et al. Coordinated optical matching of a texture interface made from demixing blended polymers for high-performance inverted perovskite solar cells. *ACS Nano*, 2020, 14, 196
- [129] Filipić M, Löper P, Niesen B, et al.  $\text{CH}_3\text{NH}_3\text{PbI}_3$  perovskite / silicon tandem solar cells: Characterization based optical simulations. *Opt Express*, 2015, 23, A263
- [130] Hossain M I, Saleque A M, Ahmed S, et al. Perovskite/perovskite planar tandem solar cells: A comprehensive guideline for reaching energy conversion efficiency beyond 30%. *Nano Energy*, 2021, 79, 105400
- [131] Liu Y, Zhang H, Zhang Y P, et al. Influence of hole transport layers on internal absorption, charge recombination and collection in  $\text{HC}(\text{NH}_2)_2\text{PbI}_3$  perovskite solar cells. *J Mater Chem A*, 2018, 6, 7922



- [132] Bisquert J, Janssen M. From frequency domain to time transient methods for halide perovskite solar cells: The connections of IMPS, IMVS, TPC, and TPV. *J Phys Chem Lett*, 2021, 12, 7964
- [133] Neukom M, Züfle S, Jenatsch S, et al. Opto-electronic characterization of third-generation solar cells. *Sci Technol Adv Mater*, 2018, 19, 291
- [134] Saranin D, Gostischev P, Tatarinov D, et al. Copper iodide interlayer for improved charge extraction and stability of inverted perovskite solar cells. *Materials*, 2019, 12, 1406
- [135] Pockett A, Carnie M J. Ionic influences on recombination in perovskite solar cells. *ACS Energy Lett*, 2017, 2, 1683
- [136] O'Regan B C, Barnes P R F, Li X E, et al. Optoelectronic studies of methylammonium lead iodide perovskite solar cells with mesoporous TiO<sub>2</sub>: Separation of electronic and chemical charge storage, understanding two recombination lifetimes, and the evolution of band offsets during J-V hysteresis. *J Am Chem Soc*, 2015, 137, 5087
- [137] Sandberg O J, Tvingstedt K, Meredith P, et al. Theoretical perspective on transient photovoltage and charge extraction techniques. *J Phys Chem C*, 2019, 123, 14261
- [138] Lei Y, Gu L Y, He W W, et al. Intrinsic charge carrier dynamics and device stability of perovskite/ZnO mesostructured solar cells in moisture. *J Mater Chem A*, 2016, 4, 5474
- [139] Chen H, Li K M, Liu H, et al. Dependence of power conversion properties of hole-conductor-free mesoscopic perovskite solar cells on the loading of perovskite crystallites. *Org Electron*, 2018, 61, 119
- [140] Tan F R, Qu S C, Jiang Q W, et al. Interpenetrated inorganic hybrids for efficiency enhancement of PbS quantum dot solar cells. *Adv Energy Mater*, 2014, 4, 1400512
- [141] Hwang D, Jin J S, Lee H, et al. Hierarchically structured Zn<sub>2</sub>SnO<sub>4</sub> nanobeads for high-efficiency dye-sensitized solar cells. *Sci Rep*, 2014, 4, 7353
- [142] Mora-Seró I, Bisquert J, Fabregat-Santiago F, et al. Implications of the negative capacitance observed at forward bias in nanocomposite and polycrystalline solar cells. *Nano Lett*, 2006, 6, 640
- [143] Boix P P, Lee Y H, Fabregat-Santiago F, et al. From flat to nanostructured photovoltaics: Balance between thickness of the absorber and charge screening in sensitized solar cells. *ACS Nano*, 2012, 6, 873
- [144] Bag M, Renza L A, Adhikari R Y, et al. Kinetics of ion transport in perovskite active layers and its implications for active layer stability. *J Am Chem Soc*, 2015, 137, 13130
- [145] Chen X Q, Shirai Y, Yanagida M, et al. Effect of light and voltage on electrochemical impedance spectroscopy of perovskite solar cells: An empirical approach based on modified randles circuit. *J Phys Chem C*, 2019, 123, 3968
- [146] Tan F R, Saidaminov M I, Tan H R, et al. Dual coordination of Ti and Pb using bilinkable ligands improves perovskite solar cell performance and stability. *Adv Funct Mater*, 2020, 30, 2005155
- [147] Yi H M, Wang D, Mahmud M A, et al. Bilayer SnO<sub>2</sub> as electron transport layer for highly efficient perovskite solar cells. *ACS Appl Energy Mater*, 2018, 1, 6027
- [148] Le Corre V M, Duijnste E A, El Tambouli O, et al. Revealing charge carrier mobility and defect densities in metal halide perovskites via space-charge-limited current measurements. *ACS Energy Lett*, 2021, 6, 1087
- [149] Khan M T, Almohammed A, Kazim S, et al. Electrical methods to elucidate charge transport in hybrid perovskites thin films and devices. *Chem Rec*, 2020, 20, 452
- [150] Liu N, Liu P, Zhou H, et al. Understanding the defect properties of quasi-2D halide perovskites for photovoltaic applications. *J Phys Chem Lett*, 2020, 11, 3521
- [151] Shi D, Adinolfi V, Comin R, et al. Low trap-state density and long carrier diffusion in organolead trihalide perovskite single crystals. *Science*, 2015, 347, 519
- [152] Zhu P C, Gu S, Luo X, et al. Simultaneous contact and grain-boundary passivation in planar perovskite solar cells using SnO<sub>2</sub>-KCl composite electron transport layer. *Adv Energy Mater*, 2020, 10, 1903083
- [153] Rothmann M U, Li W, Etheridge J, et al. Microstructural characterisations of perovskite solar cells - from grains to interfaces: Techniques, features, and challenges. *Adv Energy Mater*, 2017, 7, 1700912
- [154] Klein-Kedem N, Cahen D, Hodes G. Effects of light and electron beam irradiation on halide perovskites and their solar cells. *Acc Chem Res*, 2016, 49, 347
- [155] Edri E, Kirmayer S, Mukhopadhyay S, et al. Elucidating the charge carrier separation and working mechanism of CH<sub>3</sub>NH<sub>3</sub>PbI<sub>3-x</sub>Cl<sub>x</sub> perovskite solar cells. *Nat Commun*, 2014, 5, 3461
- [156] Fan R D, Huang Y, Wang L G, et al. The progress of interface design in perovskite-based solar cells. *Adv Energy Mater*, 2016, 6, 1600460
- [157] Edri E, Kirmayer S, Henning A, et al. Why lead methylammonium tri-iodide perovskite-based solar cells require a mesoporous electron transporting scaffold (but not necessarily a hole conductor). *Nano Lett*, 2014, 14, 1000
- [158] Yang W S, Park B W, Jung E H, et al. Iodide management in formamidinium-lead-halide-based perovskite layers for efficient solar cells. *Science*, 2017, 356, 1376
- [159] Shi J J, Xu X, Li D M, et al. Interfaces in perovskite solar cells. *Small*, 2015, 11, 2472
- [160] Wang R, Xue J, Wang K L, et al. Constructive molecular configurations for surface-defect passivation of perovskite photovoltaics. *Science*, 2019, 366, 1509



**Wanlong Wang** received his bachelor's degree from Zhengzhou University in 2019. He is currently an M.S. candidate under the supervision of Associate Professor Furui Tan at Henan University. His current research focuses on the modification of transparent electrodes for perovskite solar cells.



**Rong Liu** received her Ph.D. from School of Materials Science and Engineering, Hubei University in 2016. From 2017–2019, she worked as a postdoctoral fellow in Shenzhen Graduate School of Peking University. She joined the Henan Key Laboratory of Photovoltaic Materials, Henan University in 2019. Her current research interests include quantum dots solar cells, perovskite solar cell and photoelectric detector.